Available online at www.sciencedirect.com
ScienceDirect
Polymer 47 (2006) 7060–7069
polymer
www.elsevier.com/locate/polymer

Syntheses and specific interactions of poly(hydroxyethyl methacrylate-*b*-vinyl pyrrolidone) diblock copolymers and comparisons with their corresponding miscible blend systems

Chih-Feng Huang, Shiao-Wei Kuo*, Fang-Ju Lin, Chih-Feng Wang, Chen-Jui Hung, Feng-Chih Chang

Institute of Applied Chemistry, National Chiao Tung University, 30050 HsinChu, Taiwan

Received 29 March 2006; received in revised form 11 July 2006; accepted 31 July 2006
Available online 21 August 2006

Abstract

Combination of atom transfer radical and conventional free radical polymerizations has been successfully used to prepare poly(hydroxyethyl methacrylate-*b*-vinyl pyrrolidone) (PHEMA-*b*-PVP) copolymers with controlled molecular weight and low polydispersity (<1.4). The thermal behavior and specific interaction of PHEMA-*b*-PVP diblock copolymers and their corresponding PHEMA/PVP blends were characterized. The result shows that glass transition temperatures of diblock copolymers analysed by differential scanning calorimetry (DSC) are higher than those of the blends. Infrared and solid-state NMR spectroscopic analyses show that hydrogen-bonding interaction of hydroxyl–carbonyl groups of diblock copolymers was also greater than that of the blends. Measurement of the proton spin–lattice relaxation time in the rotating frame, ($T_{1\rho}^{H}$), reveals that all diblock copolymers and blends possess one composition-dependent $T_{1\rho}^{H}$, indicating that both diblock copolymers and blends are homogeneous, which is consistent with the DSC analysis.

Keywords: Atom transfer radical polymerization; Block copolymer; Hydrogen bonding

1. Introduction

Block copolymers composed of segments with different properties have been of considerable interest. Some fundamental research and practical technologies to clarify or improve the block copolymers have been reported [1,2]. These complex nanostructures have shown promising utilizations in environmental, biomedical, sequestration of pollutants, drug delivery, gene therapy, coatings, and composites.

Atom transfer radical polymerization (ATRP) is known to polymerize a relatively broad range of monomers such as styrenes, acrylates, and methacrylates, etc. However, not all alkenes have been successfully polymerized by ATRP including vinyl acetate, vinyl pyrrolidone, olefins, etc., presumably due to either relatively strong carbon–halogen bonds or low radical reactivities. Several efforts have been attempted to overcome this limitation to prepare related diblock copolymers. The controlled/living radical polymerizations (CRPs) were performed by combining with different polymerization methods to prepare novel block copolymers, i.e., with cationic [3], ring-opening [4], condensation [5], and anionic polymerizations [6]. Another approach is to combine CRP with conventional radical polymerization. Priddy et al. reported a method to prepare diblock copolymers by combining conventional radical polymerization and TEMPO-based CRP [7]. Destarac and Boutevin reported a similar approach by combining conventional radical polymerization and ATRP to prepare block copolymers of styrene with *n*-butyl acrylate using a difunctional initiator [8]. Matyjaszewski et al. reported four different methods to synthesize block copolymers by combining ATRP and conventional radical polymerization [9].

* Corresponding author. Tel.: +886 3 5131512; fax: +886 3 5723764.
E-mail address: kuosw@mail.nctu.edu.tw (S.-W. Kuo).

0032-3861/$ - see front matter © 2006 Elsevier Ltd. All rights reserved.
doi:10.1016/j.polymer.2006.07.071

2-Hydroxyethyl methacrylate (HEMA) is a commercially important monomer that has been widely used in the manufacture of soft contact lenses and intraocular lenses [10]. PHEMA copolymers exhibit excellent biocompatibility and good blood compatibility [11]. Other biomedical applications for PHEMA-based materials include an embedding substrate for the examination of cells using light microscopy [12], and inert matrices for the slow release of drugs [13]. Poly(vinyl pyrrolidone) (PVP) is a water-soluble tertiary amide and a strong Lewis base that also possesses good biocompatibility. Devices based on hydrogels of PVP have found several medical applications. PVP was chosen for this study because the carbonyl group is known to be a stronger hydrogen-bond acceptor than the carbonyl group of poly(methyl methacrylate) (PMMA) or the ether group of poly(ethylene oxide) (PEO).

In this article, we report the preparation of diblock copolymers of PHEMA and poly(*N*-vinyl-2-pyrrolidone) (PVP) by the combination of ATRP and conventional radical polymerization. The homopolymer of PHEMA was first prepared using ATRP from 2,2′-azobis[2-methyl-*N*-(2-(2-bromoisobutyryloxy)ethyl)propionamide] (AMBEP) initiator. At a lower polymerization temperature and carefully controlled polymerization condition to minimize the oxidation of Cu(I) to Cu(II), we were able to obtain the well-defined PHEMA homopolymer with narrow molecular weight dispersity at a reasonable rate. This initially prepared homopolymer then served as a macroinitiator to polymerize with *N*-vinyl-2-pyrrolidone (VP) monomer to form the PHEMA-*b*-PVP block copolymer by the conventional radical polymerization. It is our interest to investigate any difference in hydrogen-bonding interaction behavior between PHEMA-*b*-PVP diblock copolymers and their corresponding PHEMA/PVP blends [14] by differential scanning calorimetry (DSC), Fourier transform infrared (FT-IR) and high-resolution solid-state ^{13}C NMR spectroscopies.

2. Experimental section

2.1. Materials

2,2′-Azobis[2-methyl-*N*-(2-hydroxyethyl)propionamide] was provided by WAKO Chemicals and used as received. *N*-vinyl-2-pyrrolidone (VP) was distilled from calcium hydride and stored under N_2. 2-Hydroxyethyl methacrylate (HEMA) was distilled under reduced pressure before use. Copper(I) chloride (CuCl) was purified by washing with glacial acetic acid overnight, followed by absolute ethanol and ethyl ether, and then dried under vacuum. Triethylamine (TEA), (1-bromoethyl)benzene (BrB), 2-bromoisobutyryl bromide and 2,2′-bipyridine (bpy) were all used as received. Silica-60 gel from Merck (Germany) was used to remove the spent ATRP catalyst. All solvents were distilled prior to use. The poly(vinyl pyrrolidone) with molecular weight (M_w) of 11,000 g/mol was purchased from Acros Chemical Company, Inc.

2.2. Synthesis of difunctional initiator

The initiator was synthesized as described previously by Matyjaszewski et al. [9]. The 2,2′-azobis[2-methyl-*N*-(2-(2-bromoisobutyryloxy)ethyl)propionamide] (AMBEP) was prepared by adding 2-bromoisobutyryl bromide (5.63 mL, 4.34×10^{-2} mol) into a stirring mixture of 2,2′-azobis[2-methyl-*N*-(2-hydroxyethyl)propionamide] (5 g, 1.73×10^{-2} mol) and triethylamine (6.02 mL, 4.34×10^{-2} mol) in 150 mL of dry $CHCl_3$ in an ice bath for 1 h. After complete addition of the acid bromide, the reaction flask was stirred at room temperature for 3 h. The mixture was then transferred to a 500 mL separatory funnel and extracted consecutively with 3×200 mL of H_2O. The organic phase was dried over $MgSO_4$, filtered and the solvent was removed by rotary evaporation. The product, a white solid, was recrystallized from diethyl ether/ethyl acetate and dried under vacuum (3 g, 39.2%). ^1H NMR ($CDCl_3$), δ: 7.18 (s, 2H), 4.32 (t, 4H), 3.67 (q, 4H), 1.90 (s, 12H), 1.35 (s, 12H) ppm. Anal. Calcd for $C_{20}H_{34}Br_2N_4O_6$: C, 40.97; H, 5.84; N, 9.56. Found: C, 40.89; H, 5.90; N, 9.48.

2.3. Polymerization procedures

For a typical HEMA atom transfer radical polymerization via monofunctional initiator, $PHEMA_x$, CuCl (0.10 g, 1×10^{-3} mol) was added into a dry round-bottom flask equipped with a stir bar. After sealing the flask with a rubber septum, the flask was degassed and back-filled with nitrogen three times and then left under nitrogen. MeOH (1 mL) and HEMA (14 mL, 11.61×10^{-2} mol) were added; both were deoxygenated and added via syringes that had been purged with nitrogen. The complexing agent, bpy (0.94 g, 5.5×10^{-3} mol) in 1 mL of MeOH, was added, and the solution was stirred until the Cu complex was formed. After the complex formation, (1-bromoethyl)benzene (BrB) (0.41 mL, 3×10^{-3} mol) was added to the flask and the flask was placed at room temperature for 24 h. Purification was achieved by passing the methanolic reaction solution through a silica column to remove the Cu(II) catalyst. The blue catalyst was adsorbed onto the silica to yield a colorless aqueous solution. MeOH was evaporated by vacuum distillation to obtain concentrated mixture and the mixture was precipitated into cold diethyl ether to produce white polymer. Based on ^1H NMR analysis, conversions greater than 80% were routinely obtained. GPC analysis using DMF as eluent gave $M_n = 12{,}800$ g/mol and $M_w/M_n = 1.13$. Table 1 summarizes the characteristics of the resulting $PHEMA_x$ homopolymers.

Table 1
Summary of molecular weight data for PHEMA homopolymers (prepared via ATRP in methanol at 25 °C)

Target degree of polymerization	M_n (theory)	M_n (^1H NMR)	M_n (GPC)	M_w/M_n
$PHEMA_{30}$	4100	4200	12 800	1.13
$(PHEMA_8)_2$	2700	3000	9900	1.13
$(PHEMA_{12})_2$	3700	4400	11 400	1.15
$(PHEMA_{15})_2$	4500	5300	16 200	1.17
$(PHEMA_{34})_2$	9400	9500	19 500	1.15

For a typical HEMA atom transfer radical polymerization via difunctional initiator, $(PHEMA_y)_2$, the AMBEP initiator (0.80 g, 1.37×10^{-3} mol) and CuCl (0.27 g, 2.74×10^{-3} mol) were added to a 50-mL flask containing a stir bar. The flask was degassed and back-filled with nitrogen three times before adding deoxygenated HEMA (17 mL, 14.25×10^{-2} mol) and MeOH (20 mL) via purged syringes. After the flask was in ice bath for 10 min, the bpy (1.04 g, 5.48×10^{-3} mol) was added and the copper complex formed. After 20 min, the reaction flask was stirred at room temperature for 24 h. Purification was achieved by passing the methanolic reaction solution through a silica column to remove the Cu(II) catalyst. The blue catalyst was adsorbed onto the silica to yield a colorless aqueous solution. MeOH was removed by vacuum distillation to obtain concentrated mixture and the mixture was precipitated into cold diethyl ether to produce white polymer. Conversions greater than 70% were routinely obtained, based on ^{1}H NMR analysis. GPC analysis using DMF as eluent gave $M_n =$ 16,200 g/mol and $M_w/M_n = 1.17$. The characteristics of the resulting $(PHEMA_y)_2$ homopolymers are also summarized in Table 1.

For conventional radical polymerization of diblock copolymer, the homopolymer $(PHEMA_{34})_2$ (1.50 g, 1.58×10^{-4} mol) was added into a 50 mL flask containing a stir bar. The flask was degassed and back-filled with nitrogen three times before adding deoxygenated VP (3.50 mL, 3.20×10^{-2} mol) via purged syringes. After 20 min, the flask was placed in an oil bath set at 70 °C. After 24 h, the product was precipitated into cold ether. Conversions greater than 50% were routinely obtained, based on ^{1}H NMR analysis. GPC analysis using DMF as eluent gave $M_n = 35{,}400$ g/mol and $M_w/M_n = 1.32$. Table 2 summarizes the characteristics of the resulting PHEMA-*b*-PVP block copolymers.

2.4. Blend preparation

Desired composition containing PHEMA and PVP was dissolved in MeOH at a concentration of 5 wt% and stirred for 6–8 h. The solution was allowed to evaporate slowly at 25 °C for 1 day on a Teflon plate and dried at 90 °C for 3 days to ensure total elimination of the solvent.

2.5. Characterizations

^{1}H NMR spectra were recorded in solutions using a Bruker AM500 (500 MHz) spectrometer, with the solvent's proton signal as a standard. Elemental analysis was carried out on a Heraus CHN-rapid elemental analyzer. Molecular weights and molecular weight distribution were determined by GPC using a Waters 510 HPLC-equipped with a 410 Differential Refractometer, a UV detector, and three Ultrastyragel columns (100, 500, and 10^3 Å) connected in series in the order of increasing pore size using DMF as an eluent at a flow rate of 0.6 mL/min. The molecular weight calibration curve was obtained using polystyrene standards. Glass transition temperatures (T_gs) were measured by DSC from Du-Pont (model 910 DSC-9000 controller). Heating rate was 20 °C/min ranging 30–220 °C in nitrogen atmosphere. Approximately 4–6 mg sample was weighted and sealed in an aluminum pan. The sample was quickly cooled to 0 °C from the first scan and then scanned between 0 and 220 °C at a scan rate of 20 °C/min. The T_g was taken as the midpoint of the heat capacity transition between the upper and lower points of deviation from the extrapolated glass and liquid lines. FT-IR spectra were obtained on a Nicolet Avatar 320 FT-IR Spectrometer, 32 scans at a resolution of 1 cm^{-1} were collected with a KBr disk at room temperature. MeOH solution containing the sample was cast onto a KBr disk and dried under similar condition to that used in bulk preparation. The sample chamber was purged with nitrogen in order to maintain the film dryness. High-resolution solid-state ^{13}C NMR experiments were carried out at 25 °C using a Bruker DSX-400 Spectrometer operating at a resonance frequency of 100.47 MHz for ^{13}C. The high-resolution solid-state ^{13}C NMR spectra were acquired by using the cross-polarization (CP)/magic angle spinning (MAS)/high-power dipolar decoupling (DD) technique. A 90° pulse width of 3.9 ms with 3 s pulse delay time and an acquisition time of 30 ms with 2048 scans were used. A magic angle sample-spinning rate of 5.4 kHz was used to avoid absorption overlapping. The proton spin–lattice relaxation time in the rotating frame ($T_{1\rho}^H$) was determined indirectly via carbon observation using a 90°–τ–spin lock pulse sequence prior to CP. The data acquisition was performed at a delay time (τ) ranging from 0.1 to 12 ms with a contact time of 1 ms.

Table 2
Summary of molecular weight data for PHEMA-*b*-PVP diblock copolymers (prepared via conventional radical polymerization at 70 °C)

Copolymer composition	M_n (theory)	M_n (^{1}H NMR)	M_n (GPC)	M_w/M_n
$PHEMA_{34}$-*b*-PVP_{30}	8000	8200	16 000	1.25
$PHEMA_{34}$-*b*-PVP_{40}	9100	9200	26 500	1.26
$PHEMA_{34}$-*b*-PVP_{50}	10 200	10 400	27 900	1.25
$PHEMA_{34}$-*b*-PVP_{70}	12 400	12 400	31 600	1.27
$PHEMA_{34}$-*b*-PVP_{80}	13 500	14 000	35 400	1.32

3. Results and discussion

3.1. Polymer characterizations

Since acrylates can be polymerized in a controlled manner by ATRP at relatively low temperatures (e.g., 20 °C), the combination of conventional radical polymerization with ATRP using a difunctional initiator can be achieved. The synthetic routes of PHEMA homopolymer and PHEMA-*b*-PVP diblock copolymer are shown in Scheme 1. The synthesis strategy of the diblock copolymer includes two major steps, the PHEMA homopolymer is first synthesized by ATRP using difunctional AMBEP initiator at room temperature to avoid significant loss of the central azo functional group and the above PHEMA macroinitiator containing the central azo linkage was used in the block copolymerization with *N*-vinyl-2-pyrrolidone (VP) by conventional radical polymerization. As the fragments from the decomposition azo group of the macroinitiator,

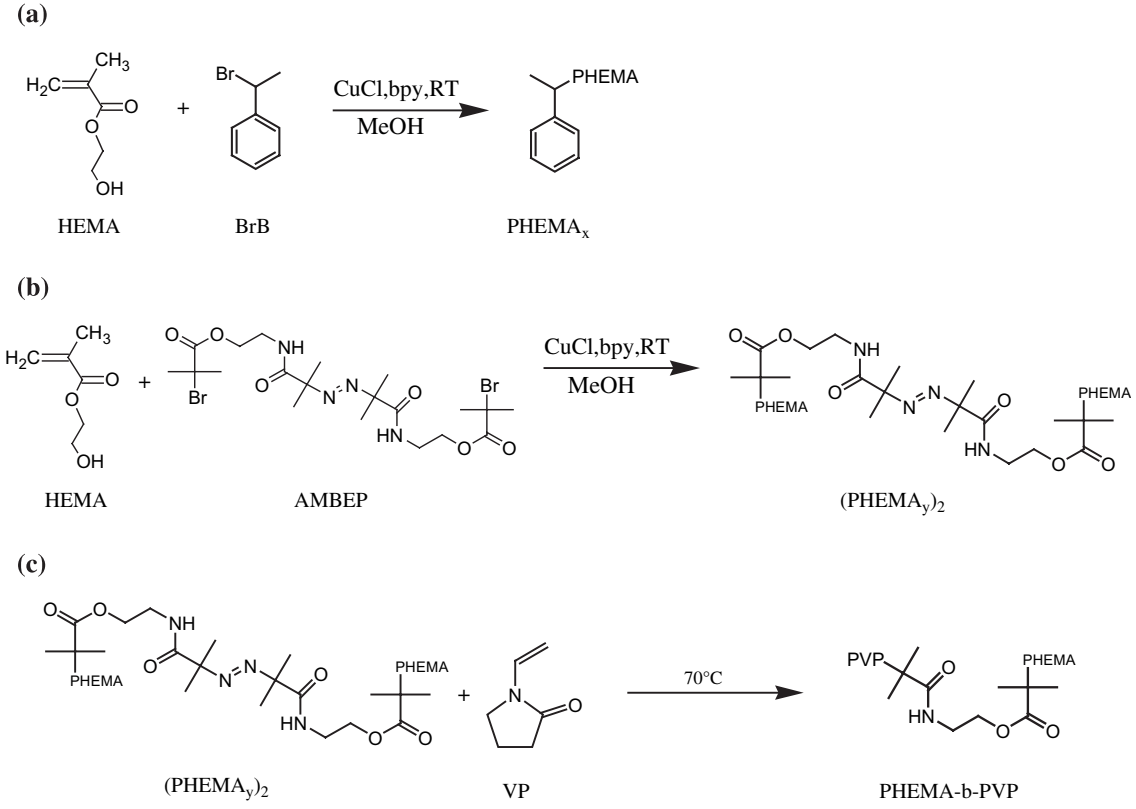

Scheme 1. The synthesis of homopolymer and diblock copolymer.

VP monomer can be incorporated into each PHEMA chain to form the PHEMA-*b*-PVP block copolymer. Additionally, we also prepared PHEMA homopolymer with monofunctional initiator of (1-bromoethyl)benzene to further compare the difference between the miscible block copolymer and its blend systems. The (1-bromoethyl)benzene is considered less likely to cause a significant "end-group" effect when assessing the water solubility of the PHEMA homopolymers (Scheme 1). Moreover, the phenyl protons also provide a useful ^{1}H NMR label for end-group analysis. These observed discrepancies between results from GPC and NMR shown in Tables 1 and 2 are probably due to the large systematic errors (200–300%) that incurred in the GPC analysis. Polystyrene calibration standards are not suitable for the analysis of methacrylic polymers. In addition, the DMF is only a marginal solvent for polystyrene, which could lead to a significant over-estimation of the true molecular weight of the well-solvated PHEMA homopolymer. This latter problem has been reported by Armes et al. [14]. The synthetic details and characterization data for various PHEMA polymers are summarized in Table 1. By comparing the GPC data obtained using this protocol with the Mn calculated from end-group analysis using ^{1}H NMR spectroscopy, we believe that the latter method is more accurate. Table 2 shows the synthetic details and characterization data for PHEMA-*b*-PVP copolymers. Their polydispersities are below 1.4, suggesting that these diblock copolymers prepared by conventional radical polymerization are controllable.

3.2. DSC analyses

The most widely used criterion for the judgment of the miscibility behavior of the diblock copolymers and the blends is the existence of a single T_g. The composition T_gs of the diblock copolymers or blends are shown in Fig. 1. All diblock copolymers and blends show composition-dependent single T_gs, implying that they are all fully miscible with a homogeneous amorphous phase. Fig. 2 shows that single T_gs of all diblock copolymers and blends are significantly higher than those predicted by Fox or Linear rule. The observed large positive deviation reveals that strong hydrogen bonding must have existed between the hydroxyl group of PHEMA and the carbonyl group of PVP. Generally, if the T_g–composition relationship is substantially deviated, neither the linear relationship nor the ideal rule of Fox is applicable. It has been generally suggested that the Kwei equation [16] is more appropriate to fit the T_g relationship to the composition of these highly deviated miscible block copolymer or polymer blends:

$$T_g = \frac{W_1 T_{g1} + kW_2 T_{g2}}{W_1 + kW_2} + qW_1 W_2 \quad (1)$$

where W_1 and W_2 are the weight fractions of the components, T_{g1} and T_{g2} represent the corresponding glass transition temperatures, and k and q are the fitting constants. In this study, $k = 1$ and $q = 185$ for the diblock copolymers and $k = 1$ and $q = 80$ were obtained for the blends from the non-linear

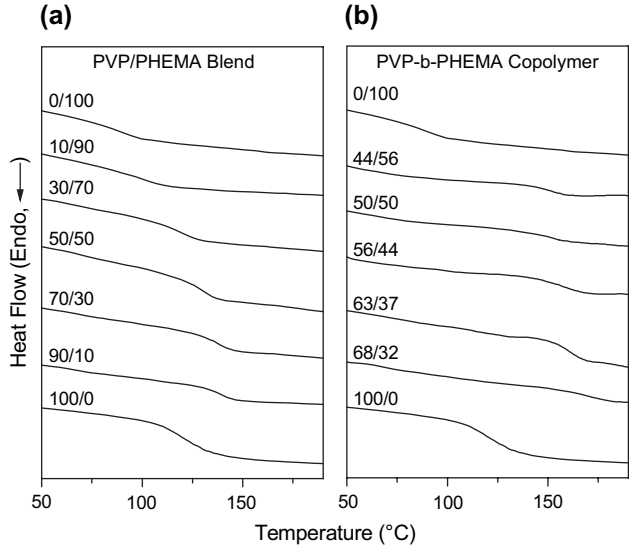

Fig. 1. The DSC curves of the (a) blends and (b) diblock copolymers with different compositions.

least-squares 'best fit' approach as shown in Fig. 2. Here q is a parameter corresponding to the strength of hydrogen bonding in the system, reflecting a balance between the breaking of the self-association and the forming of the inter-association hydrogen bonding. These observed positive q values of 185 and 80 indicate a stronger inter-association of hydrogen-bonding interaction that existed between the hydroxyl group of PHEMA and the carbonyl group of PVP than self-association hydrogen bonding of the pure PHEMA. Furthermore, the observed difference in q value from these two systems implies that the strength of the inter-association interaction within the PHEMA-*b*-PVP copolymer is greater than that of the corresponding PHEMA/PVP blend, which is also consistent with our previous studies [17,18].

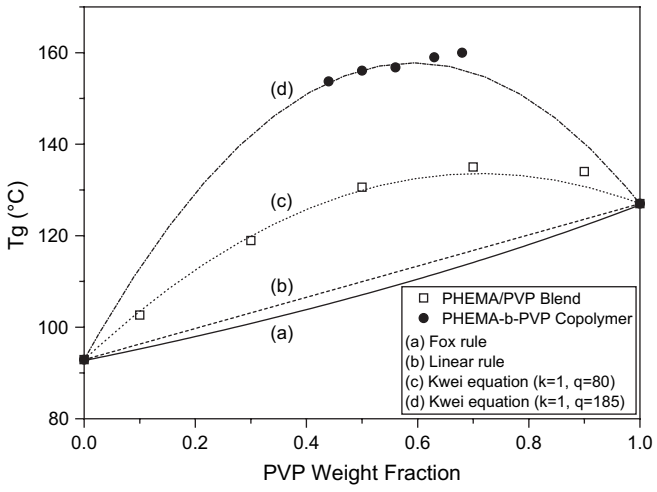

Fig. 2. The T_g vs. composition curves based on the (a) Fox rule, (b) Linear rule, (c) Kwei equation for blend systems, (d) Kwei equation for diblock copolymer systems, (■) experimental data of the blends, and (●) experimental data of the diblock copolymer systems.

3.3. FT-IR analyses

FT-IR spectroscopy has been successfully applied in numerous diblock copolymers and blends possessing intermolecular interaction through hydrogen bonding. Taking into account the chemical structure of the pure PHEMA, it possesses both proton donor of hydroxyl group and proton acceptor of carbonyl group, now, we turn our attention to the hydrogen-bonded blends in the hydroxyl stretching of PHEMA-*b*-PVP copolymers and PHEMA/PVP blend as shown in Fig. 3. The pure PHEMA shows two unresolved bands in the hydroxyl-stretching region, corresponding to the free hydroxyl at 3525 cm^{-1} and the hydrogen-bonded hydroxyl–carbonyl of the PHEMA at 3380 cm^{-1}. Fig. 3 also illustrates that the intensity of free hydroxyl group decreases gradually with the increase of the PVP content in both diblock copolymer and blend systems as would be expected. Furthermore, the intensity of the free hydroxyl group in diblock copolymers nearly disappeared at any PVP content, while, the intensity of free hydroxyl group in blends is still observable at rich PHEMA content, indicating that the copolymer system has the greatest tendency to form intermolecular hydroxyl–carbonyl hydrogen bonding. Meanwhile, the absorption of the intramolecularly hydrogen-bonded hydroxyl group with carbonyl group of PHEMA shifts to lower wavenumber with the increase of the PVP content in both systems. This result reflects a new distribution of hydrogen-bonding formation resulting from the competition between the hydroxyl–carbonyl group within the pure PHEMA and the hydroxyl–carbonyl group between PHEMA and PVP. It also reveals that interaction between PHEMA hydroxyl and PVP carbonyl becomes dominant in those PVP-rich blends. Therefore, it is reasonable to assign the bands at 3365 cm^{-1} and 3350 cm^{-1} to the hydrogen-bonding interactions between PHEMA hydroxyl and PVP carbonyl in blend and block copolymer systems, respectively. The frequency difference between the hydrogen-bonded hydroxyl absorption and the

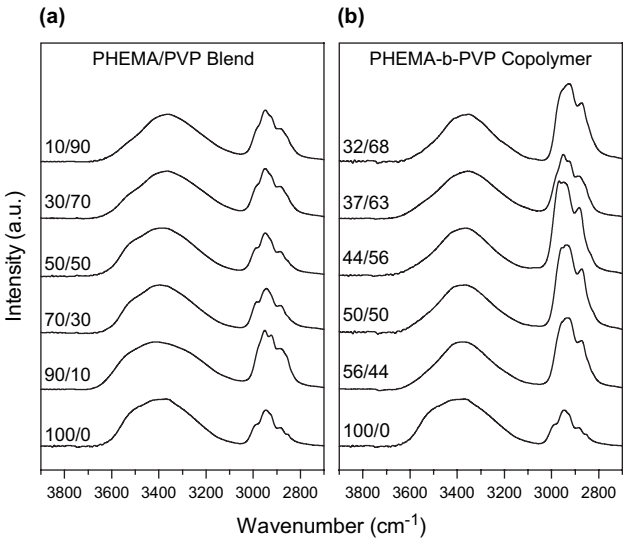

Fig. 3. FT-IR spectra at room temperature in the 2700–3900 cm^{-1} region for (a) blends and (b) diblock copolymers with different compositions.

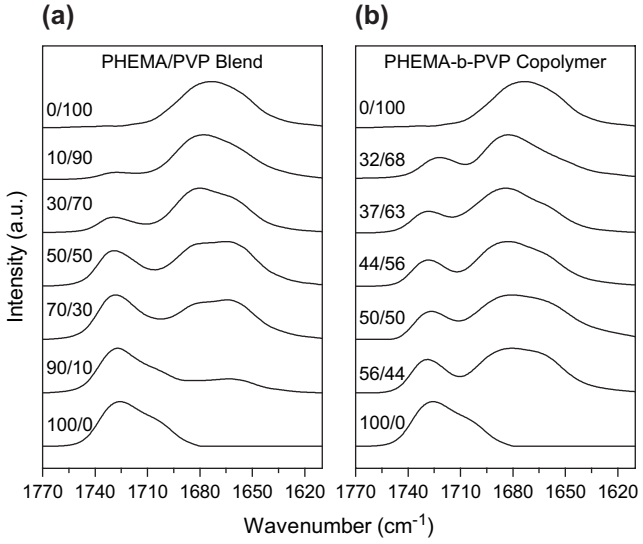

Fig. 4. FT-IR spectra at room temperature in the 1620–1780 cm^{-1} region for (a) blends and (b) diblock copolymers with different compositions.

free hydroxyl absorption ($\Delta\upsilon$) can be used to roughly estimate the average hydrogen-bonding strength and its enthalpy in a hydrogen-bonding blend system [19]. Hydrogen-bonding interactions between PHEMA hydroxyl and PVP carbonyl in both copolymer and blend systems ($\Delta\upsilon = 160$ and 175 cm^{-1}) are stronger than that of the pure PHEMA ($\Delta\upsilon = 105$ cm^{-1}) which is consistent with the observed positive q value in the Kwei equation. In addition, frequency difference in the block copolymer is also greater than that in the blend system, also indicating the stronger hydrogen-bonding interaction strength than the blend system.

Fig. 4 shows the infrared spectra of the carbonyl stretching measured at room temperature ranging from 1675 to 1765 cm^{-1} for different compositions of the diblock copolymers and the blends. Chemical structures and their IR carbonyl vibrations of the free and hydrogen-bonded PHEMA and PVP are shown in Scheme 2. The carbonyl stretching of the original PHEMA splits into two bands, absorption by the free and hydrogen-bonded carbonyl groups at 1730 and 1710 cm^{-1}, respectively. Similarly, the carbonyl stretching of PVP with increasing PHEMA content also splits into two bands at 1680 and 1665 cm^{-1}, corresponding to the free and the hydrogen-bonded carbonyl groups, respectively, that can be well fitted to a Gaussian function. The fraction of hydrogen-bonded carbonyl group of PVP can be calculated by using an appropriate absorptivity ratio ($a_R = a_{HB}/a_F = 1.3$) that has been discussed in our previous study [20,21]. Table 3 summarizes results from these curve fittings, indicating that the carbonyl

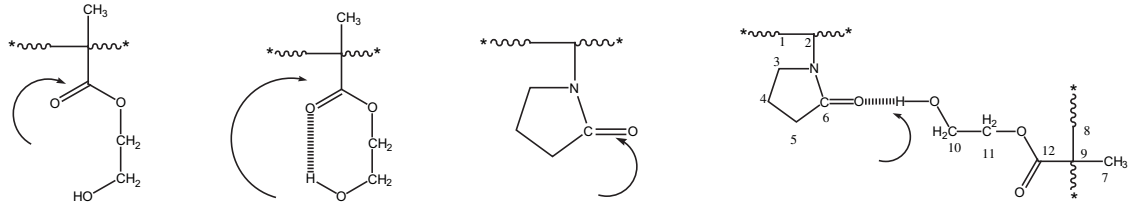

(a) Free carbonyl at 1730 cm^{-1} (b) Hydrogen-bonded carbonyl at 1710 cm^{-1} (c) Free PVP carbonyl in pure PVP homopolymer at 1680 cm^{-1} (d) Hydrogen-bonded carbonyl of PHEMA/PVP at 1665 cm^{-1}

Scheme 2. Schematic representation of PHEMA and PVP hydrogen bonding and their chemical structures of atom numbering.

Table 3
Carbonyl group curve-fitting results of the blends and diblock copolymers

	Carbonyl group of PVP					Carbonyl group of PHEMA				
	Free		H-bond		f_b	Free		H-bond		f_b
	ν_f	A_f	ν_b	A_b		ν_f	A_f	ν_b	A_b	
PHEMA/PVP										
100/0						1730	46.8	1710	53.2	43.1
90/10	1684	18.7	1663	81.3	77.1	1729	56.8	1709	43.2	33.7
70/30	1683	26.5	1663	73.5	68.2	1729	63.5	1709	36.5	27.8
50/50	1684	34.2	1661	65.8	59.7	1730	66.9	1710	33.1	24.8
30/70	1684	49.3	1663	50.7	44.2	1730	79.5	1710	20.5	14.7
10/90	1683	55.5	1660	44.5	38.1	1729	82.2	1711	17.8	12.6
PHEMA-*b*-PVP										
56–44	1688	24.7	1665	75.3	70.1	1728	63.0	1708	37.0	28.1
50–50	1688	28.6	1665	71.4	65.7	1728	65.4	1708	34.6	26.6
44–56	1688	38.3	1666	61.7	55.2	1728	69.2	1710	30.8	22.8
37–63	1688	43.8	1668	56.2	49.6	1730	81.5	1710	18.5	13.1
32–68	1687	45.0	1668	55.0	48.4	1723	91.0	1708	9.0	6.1

ν_f: wavenumber of free C=O (cm^{-1}); ν_b: wavenumber of hydrogen-bonded C=O; A_f: area percent of free C=O; A_b: area percent of hydrogen-bonded C=O. f_b: percent of hydrogen-bonded C=O.

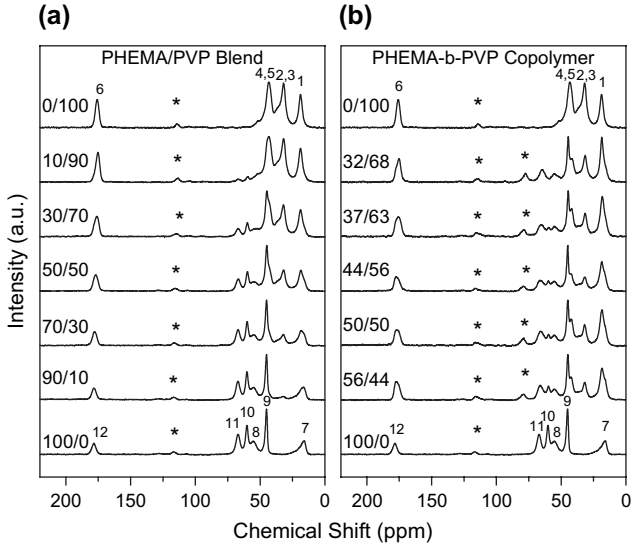

Fig. 5. ^{13}C CP/MAS NMR for (a) blends and (b) diblock copolymers with different compositions (weight ratio).

hydrogen-bonded fraction of PVP increases with the increase of the PHEMA content in both diblock copolymer and blend systems and the hydrogen-bonded carbonyl fraction of PHEMA will decrease with the increase of PVP content because most hydroxyl groups of the PHEMA will interact with the carbonyl of PVP as shown in Fig. 3. In addition, the fraction of hydrogen-bonded carbonyl group of PVP at same PHEMA weight fraction (50/50) reveals that the hydrogen-bonding interaction of the diblock copolymers is greater than that of the blends and these results are consistent with previous Kwei equation.

Table 4
Chemical shifts (ppm) observed in the ^{13}C CP/MAS/DD NMR spectra of PHEMA and PVP units in their block copolymers and polymer blends

PHEMA/PVP	PVP			
	C-1	C-2, C-3	C-4, C-5	C-6
Pure PVP	18.9	31.9	43.5	175.0
10/90	18.7	31.9	43.5	175.2
30/70	18.7	32.0	44.8	175.8
50/50	18.6	32.0	44.8	177.2
70/30	18.4	32.1	45.1	177.5
90/10	–	–	45.1	177.9

	PHEMA				
	C-7	C-8, C-9	C-10	C-11	C-12
10/90	15.7	43.5	–	–	175.2
30/70	15.7	44.8	59.8	66.7	175.8
50/50	15.7	44.9	59.8	66.7	177.2
70/30	15.7	45.1	60.0	67.0	177.5
90/10	15.7	45.1	60.1	67.2	177.9
Pure PHEMA	15.7	45.1	60.2	67.2	178.3

PHEMA-*b*-PVP	PVP			
	C-1	C-2, C-3	C-4, C-5	C-6
33/67	18.7	31.4	44.5	175.2
37/63	18.4	31.5	44.5	175.9
44/56	18.7	31.7	44.9	176.7
50/50	18.6	31.9	44.9	178.0
56/44	18.5	31.9	44.9	178.2

	PHEMA				
	C-7	C-8, C-9	C-10	C-11	C-12
33/67	15.7	44.5	59.3	64.7	175.2
37/63	15.7	44.5	59.5	65.4	175.9
44/56	15.7	44.9	59.8	65.7	176.7
50/50	15.7	44.9	59.8	66.0	178.0
56/44	15.7	44.9	59.8	66.2	178.2

3.4. Solid-state NMR analyses

In addition to FT-IR, evidences on interactions in the diblock copolymers and the blends can also be obtained from solid-state NMR spectroscopy as demonstrated by the changes in chemical shift and/or line shape. Fig. 5 shows the selected ^{13}C CP/MAS spectra of various PHEMA-*b*-PVP copolymers and PHEMA/PVP blends. The pure PHEMA displays six peaks where the carbonyl atom (C-12) is at $\delta = 178.3$ ppm and the CH_2–OH carbon atom (C-10) is at $\delta = 67.2$ ppm. Six peaks are also observed for pure PVP where the peak at $\delta =$ 175.0 ppm corresponds to the carbonyl carbon atom (C-6). All other peaks designated in Fig. 5 are assigned in Scheme 2(d). Table 4 summarizes the values of the chemical shifts observed in the ^{13}C CP/MAS NMR spectra of PHEMA/PVP blends and PHEMA-*b*-PVP copolymers. Compared with the ^{13}C CP/MAS NMR spectra of the pure PHEMA and PVP with the spectra of the blends and copolymers, significant

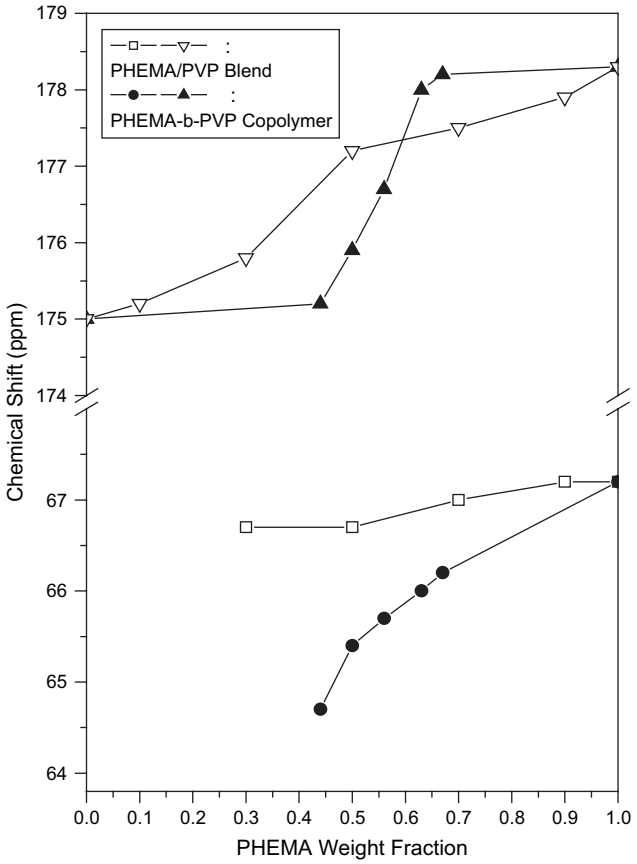

Fig. 6. ^{13}C CP/MAS NMR chemical shift of 65 and 178 ppm with different compositions.

changes were observed, especially for the resonances of those carbon atoms that are involved in intermolecular interactions. Fig. 6 shows chemical shift resonances of CH_2OH (C-10) and carbonyl carbons (C-12) of the PHEMA and the carbonyl carbon (C-6) of PVP against the PHEMA content. Clearly, the signals of the CH_2OH group of PHEMA shift upfield upon increasing the PVP content in both the blend and copolymer systems. This result is consistent with previous studies suggesting the existence of specific interactions between PHEMA and PVP. Furthermore, the chemical shift of the diblock copolymer is greater than the corresponding blend system, also indicating that the diblock system has the stronger interaction than the blend. However, based on the chemical shifts of carbonyl carbons from the PVP and PHEMA in the diblock copolymers and blends, it is still difficult to differentiate the strength of hydrogen-bonding interaction between the diblock and blend systems. In order to confirm the existence of the hydrogen-bonding interaction involving the carbonyl group in PHEMA-*b*-PVP copolymers and PHEMA/PVP blends by solid-state NMR spectra, the experimental and the simulated data are shown in Fig. 7, which are similar to our previous study about the poly(methyl methacrylate-*co*-methylacrylamide) copolymer system [22]. The simulated spectra for copolymers and blends are obtained from simple sum of each experimental ^{13}C NMR spectrum of pure PHEMA and pure PVP at the respective molar ratio and they are shown in the right hand side. Fig. 7 shows that the experimental spectra of block copolymers and blends differ noticeably from the simulated spectra, implying that the hydrogen bonding exists between the hydroxyl group of PHEMA and the carbonyl group of PVP. We can realize that the hydrogen-bonding interaction between the copolymer and blend systems is quite different, only one single peak is present in blend system but two peaks are shown in copolymer system. According to earlier FT-IR analyses, four

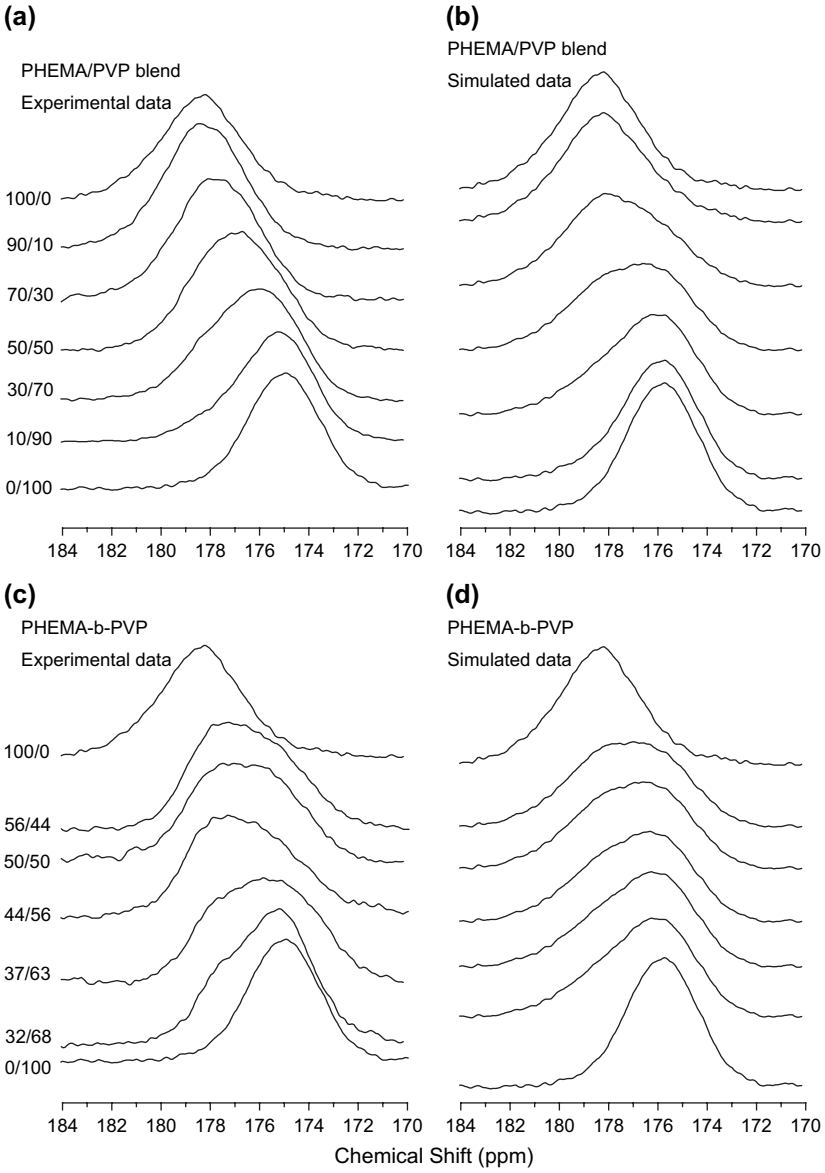

Fig. 7. Experimental and simulated data of ^{13}C CPMAS spectra at room temperature (a) and (b) for blends, (c) and (d) for diblock copolymers.

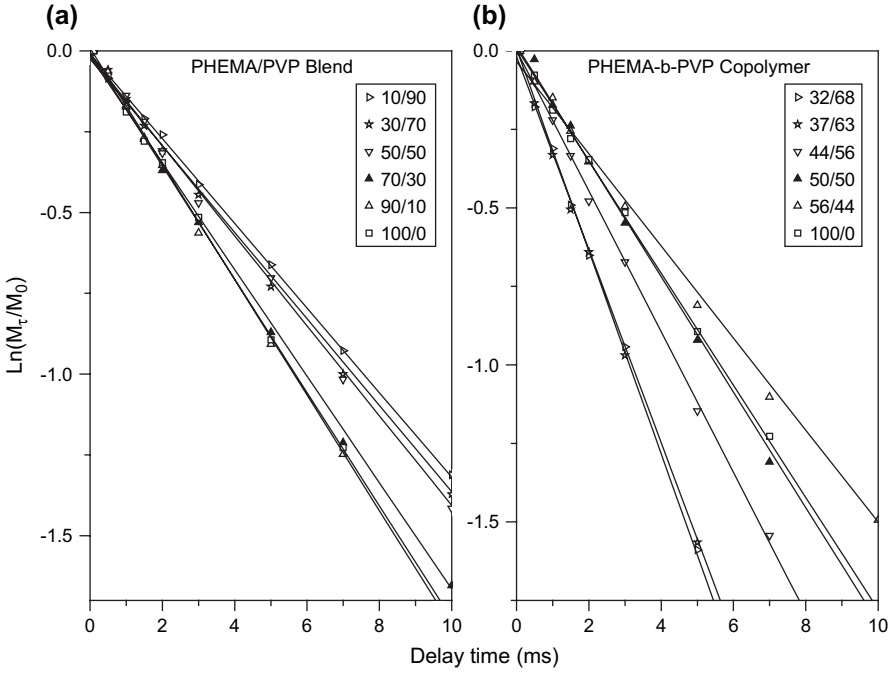

Fig. 8. Logarithmic plots of the intensities of 60 ppm vs. delay time for (a) blends and (b) diblock copolymers with different compositions.

types of carbonyl situations are possible: (1) free carbonyl group of PHEMA, (2) self-associating hydrogen-bonded carbonyl group of PHEMA, (3) free carbonyl group of PVP, and (4) intermolecular hydrogen-bonded carbonyl group of PVP with PHEMA. For the carbonyl carbon of PHEMA, the carbonyl shifts upfield with increasing PVP content while the free carbonyl carbon appears at higher PVP content or at stronger intermolecular hydrogen bonding of PVP carbonyl with PHEMA hydroxyl. On the contrary, the carbonyl carbon of PVP shifts downfield with the increase of PHEMA content. In the blend system, the carbonyl group shows single peak since the upfield shift of the PHEMA carbonyl is overlapped with the downfield shift of the PVP carbonyl. However, in the relatively stronger hydrogen-bonding copolymer system, the larger upfield shift of the PHEMA carbonyl can be separated from the larger downfield shift of the PVP carbonyl, so that two peaks in copolymer system can be observed. Therefore, solid-state NMR is able to provide additional evidence that the hydrogen-bonding strength in copolymer system is indeed greater than that in the blend system.

Solid-state NMR spectroscopy has been used to better understand the phase behavior and miscibility of the diblock copolymers and the blends. A single T_g based on DSC analysis implies that the mixing of two blending components is in a scale of about 20–40 nm [23]. The dimension of mixing smaller than 20 nm can be obtained through measurement of the spin–lattice relaxation time in the rotating frame ($T_{1\rho}^{H}$) [23]. The $T_{1\rho}^{H}$ values of the blends and copolymers were measured through the delayed-contact ^{13}C/MAS experiments. The $T_{1\rho}^{H}$ values are calculated from Eq. (2):

$$\ln(M_\tau/M_0) = -\tau/T_{1\rho}^{H} \tag{2}$$

where τ is the delay time used in the experiment, and M_τ is the corresponding resonance.

Fig. 8 shows plots of $\ln(M_\tau/M_0)$ vs. τ, for the PHEMA resonance (60 ppm) in the diblock copolymers and the blends. The experimental data are in good agreement with Eq. (2). From the slope of the fitting line, the $T_{1\rho}^{H}$ value can be determined. Table 5 lists the results of the $T_{1\rho}^{H}$ values for the diblock copolymers and the blends.

A single composition-dependent $T_{1\rho}^{H}$ was obtained for each of the diblock copolymers and the blends where $T_{1\rho}^{H}$ values of the blends are intermediate between those two pure polymers, while $T_{1\rho}^{H}$ values of the diblock copolymer are above that of the pure PVP. It suggests that both diblock copolymers and the blends are homogeneous to a scale where the spin-diffusion occurs within the time $T_{1\rho}^{H}$.

The upper spatial scale of the spin-diffusion path length L can be estimated from the following expression [24]:

$$L = \left(6DT_{1\rho}^{H}\right)^{1/2} \tag{3}$$

Table 5
Relaxation time, $T_{1\rho}^{H}$, and domain size for (a) blends and (b) diblock copolymers at the magnetization intensities of 67 ppm

(a) PHEMA/PVP	$T_{1\rho}^{H}$ (ms)	(b) PHEMA-*b*-PVP	$T_{1\rho}^{H}$ (ms)
100/0	5.59	100/0	5.59
90/10	7.63	56/44	6.81
70/30	7.46	50/50	5.43
50/50	7.18	44/56	4.46
30/70	6.06	37/63	3.25
10/90	5.71	33/67	3.10
0/100	8.28	0/100	8.28

where D, which is typically assumed to be 10^{-16} m^2 s^{-1}, is the effective spin-diffusion coefficient depending on the average proton to proton distance as well as the dipolar interaction (Table 4). Therefore, the upper limit of the domain sizes for the blends is estimated to be 1.2–1.6 nm while that of the diblock copolymers is estimated to be 0.9–1.5 nm. It can be seen that the diblock copolymers have relatively smaller domain sizes than the corresponding blends, indicating that the degrees of homogeneity of the diblock copolymers are relatively higher than those of the blends. By comparing the polymer blend of poly(acrylic acid) (PAA)/poly(vinyl pyrrolidone) (PVP) with the complex PAA/PVP, the resultant $T_{1\rho}^{H}$ values show that the complex PAA/PVP is shorter than the corresponding blend [25]. As a result, we proposed that the polymer chain behavior of PHEMA/PVP blend is separated coils, but increasing the hydrogen-bonding strength for PHEMA-*b*-PVP diblock copolymer, polymer complex aggregate is proposed. Spin–lattice relaxation time in the rotating frame ($T_{1\rho}^{H}$) based on solid-state NMR analysis is able to provide positive evidence that polymer complex aggregate in the diblock copolymer has the shorter $T_{1\rho}^{H}$ value than the separated coils in the miscible blend.

4. Conclusions

In this study, we have successfully synthesized diblock copolymers of PHEMA with PVP. From DSC analyses, we observed higher glass transition temperatures for PHEMA-*b*-PVP copolymers relative to their corresponding PHEMA/PVP blends as a result of stronger specific interactions existing in the former copolymer system. FT-IR and solid-state NMR spectroscopic analyses provided evidence that the specific interaction in the PHEMA-*b*-PVP copolymer arises from the hydroxyl group of PHEMA and the carbonyl group of PVP, similar to that observed for the PHEMA/PVP blend system. Measurements of $T_{1\rho}^{H}$ reveal that all systems possess a single composition-dependent $T_{1\rho}^{H}$, indicating that all diblock copolymers and blends are in homogeneity. Moreover, the calculated domain sizes of the diblock copolymers are relatively smaller than the corresponding blends.

Acknowledgements

The authors would like to thank the National Science Council, Taiwan, Republic of China for financially supporting this research under Contract Nos. NSC-95-2216-E-009-001 and Ministry of Education "Aim for the Top University" program (MOEATU program).

References

[1] Peppas NA, editor. Hydrogel in medicine and pharmacy, vol. 2. Boca Raton, FL: CRC Press; 1987.
[2] Nagaoka S, Mori Y, Tanzawa H, Kikuchi Y, Inagaki F, Yokota Y, et al. ASAIO Trans 1987;10:76.
[3] Yagci Y, Duz AB, Onen A. Polymer 1997;38:2861.
[4] Coca S, Paik HJ, Matyjaszewski K. Macromolecules 1997;30:6513.
[5] Gaynor SG, Matyjaszewski K. Macromolecules 1997;30:4241.
[6] Yoshida E, Tanimoto S. Macromolecules 1997;30:4018.
[7] Li IQ, Howell BA, Dineen MT, Kastl PE, Lyons JW, Meunier DM, et al. Macromolecules 1997;30:5195.
[8] Destarac M, Pees B, Bessiere JM, Boutevin B. Polym Prepr 1998;39(2):566.
[9] Paik HJ, Teodorescu M, Xia J, Matyjaszewski K. Macromolecules 1999;32:7031.
[10] Menace R, Skorpik C, Juchem M, Scheidel W, Schranz RJ. J Cataract Refract Surg 1989;15:264.
[11] Seifert LM, Green RT. J Biomed Mater Res 1985;19:1043.
[12] Bennet HS, Wyricks AD, Lee SW, McNeil HJ. Stain Technol 1976;51:71.
[13] Canal T, Peppas NA. J Biomed Mater Res 1989;23:1183.
[14] Weaver JVM, Bannister I, Robinson KL, Bories-Azeau X, Armes SP. Macromolecules 2004;32:7031.
[16] Kwei TK. J Polym Sci Polym Lett Ed 1984;22:307.
[17] Lin CL, Chen WC, Liao CS, Su YC, Huang CF, Kuo SW, et al. Macromolecules 2005;38:6435.
[18] Kuo SW, Huang CF, Tung PH, Huang WJ, Huang JM, Chang FC. Polymer 2005;46:9348.
[19] Moskala EJ, Varnell DF, Coleman MM. Polymer 1985;26:228.
[20] Kuo SW, Chang FC. Macromolecules 2001;34:5224.
[21] Kuo SW, Shih CC, Shieh JS, Chang FC. Polym Int 2004;53:218.
[22] Kuo SW, Kao HC, Chang FC. Polymer 2003;44:6873.
[23] Kuo SW, Chang FC. Macromolecules 2001;34:4189.
[24] McBrierty VJ, Douglass DC. J Polym Sci Macromol Rev 1981;16:295.
[25] Lau C, Mi Y. Polymer 2002;43:823.